RESEARCH ARTICLE

WILEY

Peak-over-threshold: Quantifying ground motion beyond design

Pasquale Cito | Iunio Iervolino ®

Dipartimento di Strutture per l'Ingegneria e l'Architettura, Università degli Studi di Napoli Federico II, Naples, Italy

Correspondence
Iunio Iervolino, Dipartimento di Strutture per l'Ingegneria e l'Architettura, Università degli Studi di Napoli Federico II, Naples, Italy.
Email: iunio.iervolino@unina.it

SUMMARY

In performance-based seismic design, as adopted by several building codes worldwide, the structural performance is verified against ground motions that have predetermined exceedance return periods at the site of interest. Such a return period is evaluated by means of probabilistic seismic hazard analysis (PSHA), and the corresponding ground motion is often represented by the uniform hazard spectrum (UHS). The structural performance for ground motions larger than those considered in this design approach is, typically, not explicitly controlled under the assumption that they are sufficiently rare. On one hand, this does not achieve uniform safety at sites characterized by different design ground motions corresponding to the same return period; on the other hand, exceedances of the design spectra are systematically observed over large areas, for example in Italy. The latter issue is because of the nature of UHS, the exceedance of which is likely-to-almost-certain when the construction site is in the epicentral area of moderate-to-high magnitude earthquakes (ie, the design spectrum may be not conservative at these locations), especially if PSHA is based on seismic source zones. The former is partially because of the systematic difference of ground motions for return periods larger than the design one at the different sites. Quantification of the expected ground motion given the exceedance of the design ground motions (ie, the recently introduced as the expected *peak-over-threshold* or POT) can be of help in quantitatively assessing these issues. In the study, a procedure to compute the POT distribution is derived first; second, POT spectra are introduced and used to help understanding why and how seismic structural reliability of code-conforming structures decreases as the seismic hazard of the site increases; third, expected and 95th percentile POT maps are shown for Italy to discuss how much high hazard sites are exposed to much larger peak-over-threshold with respect to mid-hazard and low-hazard sites; finally the POT is discussed with respect to the slope of the hazard curve (in log-log scale) at the threshold, a known proxy for ground motion beyond design. All data presented in the maps are made available for the interested reader as a supplemental archive.

KEYWORDS
limit state, performance-based earthquake engineering, seismic reliability, spectrum

1 | INTRODUCTION

According to the performance-based seismic design paradigm,[1] as acknowledged by several contemporary building codes such as the Italian code or the Eurocode 8 (EC8),[2] seismic actions derive from probabilistic seismic hazard analysis or PSHA.[3,4] In fact, in most worldwide codes, design ground motion (GM) is represented in terms of the uniform hazard spectrum (UHS), that is, a spectrum with ordinates that, taken individually, have the same probability of being exceeded in a given time interval or, equivalently, same return period of exceedance (T_r). The return period used for design depends on the performance of interest; ie, the *limit state.* Because the structural performance for GM larger than the design one is not controlled, the return period is chosen so that exceedance is sufficiently rare to be acceptable. A typical number for the *life-safety* limit state, according to the Italian code, is $T_r = 475yr$ that corresponds to the *significant-damage* limit state according to EC8.

Exceedances of code spectra based on UHS are systematically observed over large areas, for example, in all the damaging earthquakes occurring in the last 10 years in Italy.[5] Dedicated studies clarified that exceedance of design spectra is expected to be rare only from the perspective at one individual site (eg, once every 475 years at that site), while it is as more frequent as larger the number of considered sites is. Moreover, it has been demonstrated that exceedance of design spectra is likely-to-almost-certain in the epicentral area of earthquakes of moderate-to-high magnitude, especially when the hazard assessment is based on seismic source zones. For example, would an earthquake of magnitude about six to occur anywhere in Italy, a site within 5 km would likely see its peak ground acceleration (PGA) with $T_r = 475$ years exceeded.[6] This happens also in regions where the maximum magnitude considered in the hazard assessment is about 7.5. The consequence of engineering interest is that it is systematically expected that the structures in the epicentral areas of moderate-to-high earthquakes must withstand seismic actions larger than those accounted for by design. Roughly speaking, one can iconoclastically say that the design spectrum *does not protect* in the epicentral areas of these events.

It is well-known that this issue has a reflection on seismic structural reliability so that buildings of the same typology, designed for the same limit state at different sites, characterized by different design GM corresponding to the same return period of exceedance, have annual failure rates that can be different by orders of magnitude.[7-9] Although this is partially because the way design actions translate in seismic resistance according to modern seismic codes, as it is well known, there is also an effect of GM corresponding to return periods larger than the design one, and against which structural performance is not verified.

For both issues* discussed so far (that are not unrelated each-other), it could be useful to compute the expected GM in earthquakes exceeding the design seismic action; ie, to quantify the extra-intensity the structures are exposed to in these events. To this aim, the expected value of the peak-over-threshold (POT) has been recently introduced.[10] It is the mean spectral (pseudo) acceleration conditional to the exceedance of a threshold value (ie, the code spectrum). It has been shown that it can be computed via disaggregation[11] of the seismic hazard analysis the design UHS descends from; thus, it is consistent with it.

Mapping the expected POT for Italy allowed the observation that: (a) it significantly varies over the country; (b) the larger expected POT values are observed where the *epsilon* (ε) from disaggregation is lower and vice-versa; (c) it can be larger than twice the design spectral ordinate it refers to, meaning that the exposure, beyond the design spectrum, of structures in the epicentral areas of *strong earthquakes* (ie, those exceeding the design GM), can be large.

Starting from these conclusions, the study presented herein is intended to introduce some extensions and further results. First, the full POT distribution is introduced, and it is shown how it can be computed from the hazard curve for the site, without the need to recur to hazard disaggregation. Then, it is discussed how the moments of the POT distribution change with the return period of the threshold, the site's hazard, and the vibration period of the spectral ordinate being considered. Uniform and conditional-POT spectra are also introduced. The effect of the POT on seismic structural reliability is quantified and discussed. Finally, because the local slope of the hazard curve at the intensity corresponding to the median capacity is related to the seismic structural reliability,[12] it is also discussed that the POT is more informative than the slope of the hazard curve, although being computable with the same input information, thus also preferable.

---

*Although design based on *risk-targeted ground motions*[7] should solve the issue, as it aims at choosing the design actions to achieve a predefined seismic safety, it is not yet widespread in codes (except some attempts), and the design approach based on fixed return periods will be likely still grounded in practice for quite some time. It also should be mentioned, for completeness, that the risk-targeted approach has its own issues, mostly related to the required assumptions on the seismic fragility of the structure to be designed.

The remainder of the paper is structured such that what is likely to happen, in terms of seismic action, in the epicentral areas of moderate-to-high magnitude earthquakes, is recalled first. Subsequently, the procedure to obtain the POT distribution is derived and discussed for three sites exposed to low-hazard, mid-hazard, and high-hazard in Italy, along with the POT spectra. Six-story reinforced concrete moment resisting frames are considered to assess the effect of the POT on the structural safety and to discuss possible viable options within the considered design approach. Finally, the expected value and the 95th percentile of the POT are mapped for Italy considering three return periods of design interest. These maps, based on data made accessible for the reader, are discussed with respect to the corresponding maps of the hazard curve's slope at the threshold. Final remarks close the study.

2 | PSHA AND EPICENTRAL AREAS

Preliminarily to introduce the POT distribution, and to understand why it could be meaningful for earthquake engineering, it must be recalled what is likely to happen for PSHA-based seismic actions in epicentral areas.

If the considered GM intensity measure is the spectral acceleration, $Sa(T)$, at a vibration period of interest, T, and referring to some damping factor, the main result of PSHA is the rate of seismic events ($\lambda_{Sa(T) > sa}$) exceeding a threshold value (sa) at the site of interest. Such a rate, which completely defines the homogeneous Poisson process regulating the occurrence of earthquakes causing the exceedance of sa over time,[3] can be computed as per Equation (1), that is the *hazard integral*, which is written assuming that the site is subjected to earthquakes from s sources:

$$\lambda_{Sa(T) > sa} = \sum_{i=1}^{s} \nu_i \cdot \int_{r_{min}}^{r_{max}} \int_{m_{min}}^{m_{max}} P[Sa(T) > sa \mid m, r] \cdot f_{M,R,i}(m,r) \cdot dm \cdot dr. \tag{1}$$

In the equation, the $i = \{1,2,...,s\}$ subscript denotes the *i-th* seismic source, which is characterized by the rate of earthquakes, ν_i, above a minimum magnitude (M) of interest (m_{min}) and below the maximum magnitude deemed possible for the *i-th* source (m_{max}). The term $f_{M,R,i}(m,r)$ represents the joint probability density function (PDF) of magnitude and source-to-site distance (R). The (r_{min}, r_{max}) interval contains the possible values of the distance of the earthquake, occuring on the *i-th* source, from the site. Finally, $P[Sa(T) > sa \mid m,r]$ is the probability of exceeding the sa threshold given magnitude and distance, and it is typically provided by a ground-motion prediction equation (GMPE). In their classical format, GMPEs model the logarithm of $Sa(T)$ as per Equation (2):

$$\log[Sa(T)] = \mu_{Sa(T),m,r} + \theta_{Sa(T)} + \sigma_{Sa(T)} \cdot \varepsilon, \tag{2}$$

in which $\mu_{Sa(T),m,r} + \theta_{Sa(T)}$ is the mean of $\log[Sa(T)]$ given $\{M,R,\theta_{Sa(T)}\}$, and $\theta_{Sa(T)}$ denotes one or more coefficients accounting for other features (eg, the soil type); $\sigma_{Sa(T)} \cdot \varepsilon$ is a zero-mean and $\sigma_{Sa(T)}^2$ variance Gaussian random variable; ie, ε is the *standardized residual* of the GMPE.

Computing Equation (1) for different threshold values allows obtaining the curve of the rates of exceedance as a function of sa, that is the hazard curve for the site. To help the discussion, this study considers three sites, at comparatively low-hazard, mid-hazard, and high-hazard in Italy (ie, Milan, Naples, and L'Aquila, respectively). Figure 1 (right)
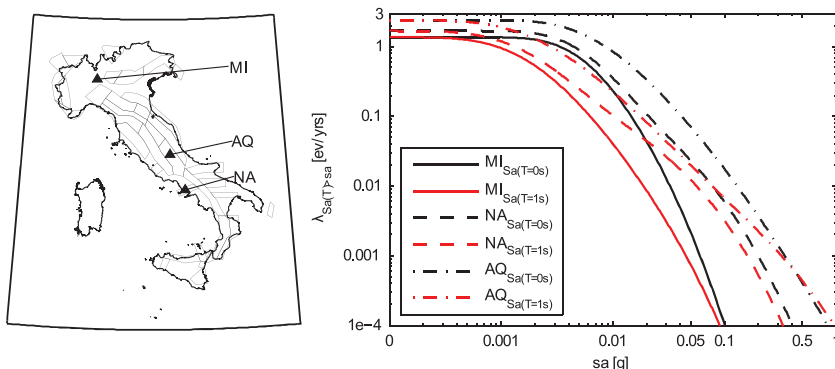

FIGURE 1 Left: three sites considered for the analyses herein; right: hazard curves for two spectral ordinates [Colour figure can be viewed at wileyonlinelibrary.com]

shows the PGA, that is $Sa(T = 0s)$, and $Sa(T = 1s)$ hazard curves for the sites (5% damping factor is considered). The different shape of the hazard curves can be appreciated. It has a direct effect on what discussed in the following.

The curves, as well as all other results shown hereafter, were obtained considering the seismic source zones described in the study that lies at the basis of the definition of the structural seismic actions according to the code enforced in the country.[13] Such a study features a logic tree made of several branches; herein, the branch identified as 921 was used. It considers the seismic source model of Meletti et al,[14] which is made of 36 areal seismic zones, numbered from 901 to 936 (depicted in Figure 1, left). The seismicity of each zone is represented by the annual rates of earthquake occurrence associated to bins of *surface-wave mangitude*.[15] The considered GMPE is that of Ambraseys et al,[16] which was applied between magnitude 4.0 and 7.5 and epicentral distance up to 230 km. Assuming a uniform epicenter distribution in each seismic source zone, epicentral distance was converted into the *Joyner and Boore* distance[17] (ie, the metric adopted by the GMPE) according to Montaldo et al.[18] In order to account for the predominant style-of-faulting of each seismic source, the correction factors proposed by Bommer et al[19] were also applied. The hazard was computed using the REASSESS software presented in Chioccarelli et al.[20]

2.1 | Exceedance scenarios

It is useful to recognize that the product $\nu_i \cdot f_{M,R,i}(m,r) \cdot dm \cdot dr$ is the rate of earthquakes, from the i-th source, that come from the $M \in (m, m+dm)$ and $R \in (r, r+dr)$ bins. Therefore, the hazard integral can be rewritten in finite terms as:

$$\lambda_{Sa(T) > sa} \approx \sum_{i=1}^{s} \sum_{m_{\min}}^{m_{\max}} \sum_{r_{\min}}^{r_{\max}} P[Sa[T] > sa \mid m,r] \cdot \nu_{m,r,i} \cdot \Delta r \cdot \Delta m, \tag{3}$$

where summations replace integrals as computations require finite bins, Δr and Δm, in lieu of dr and dm.

In fact, even the product $P[Sa(T) > sa \mid m,r] \cdot \nu_{m,r,i} \cdot \Delta r \cdot \Delta m$ is a rate. It is the mean number of earthquakes per unit-time from the *i*-th source that cause exceedance of the *sa* threshold and come from the $\{m,r\}$ bin. Such a rate can be indicated as $\lambda_{Sa(T) > sa,m,r,i} \cdot \Delta r \cdot \Delta m$. Thus, the hazard integral reduces to:

$$\lambda_{Sa(T) > sa} \approx \sum_{i=1}^{s} \sum_{m_{\min}}^{m_{\max}} \sum_{r_{\min}}^{r_{\max}} \lambda_{Sa(T) > sa,m,r,i} \cdot \Delta r \cdot \Delta m. \tag{4}$$

This representation is useful: Figure 2 shows the hazard integral to compute the rate of exceedance of $Sa(T = 1s)$, on rock soil conditions, that corresponds to $T_r = 475yr$ at the site of L'Aquila (central Italy), that is, $sa_{T_r = 475} = 0.21g$.

The left panel of the figure provides the $\nu_{m,r} \cdot \Delta r \cdot \Delta m$ rates for all the sources within 230 km from the site (in terms of epicentral distance), while the central panel gives $P[Sa(T) > sa_{T_r = 475} \mid m,r]$. The product of the two leads to the right panel which is $\lambda_{Sa(T) > sa_{T_r = 475},m,r} \cdot \Delta r \cdot \Delta m$. It is clear, by definition, that summing up the values in the right panel yields $1/475 = 0.0021$.
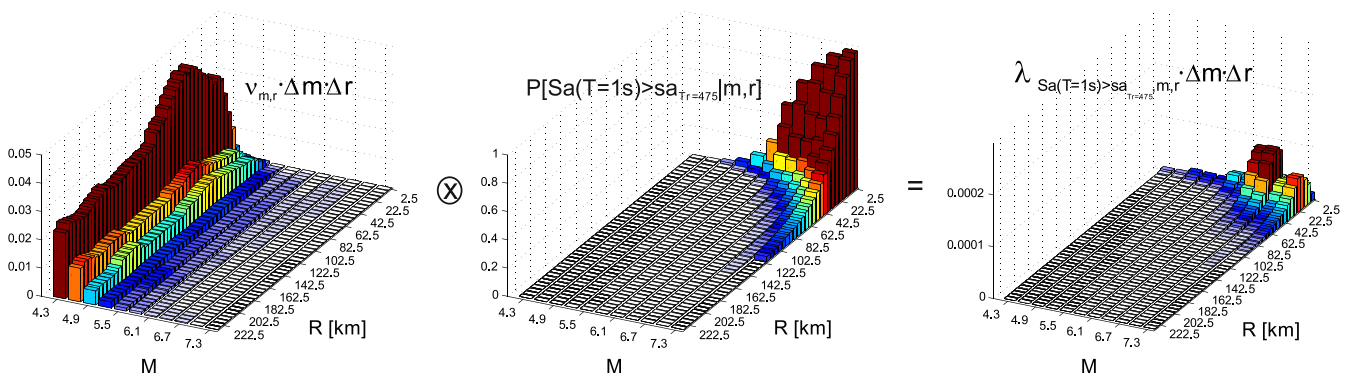

FIGURE 2 Hazard terms for the 1-second spectral acceleration with 475-year exceedance return period in L'Aquila. Left: occurrence rates per magnitude and distance bins; center: probability of exceedance from the GMPE; right: rates of earthquakes exceeding the threshold from specific magnitude-distance bins[6]

It can be seen from the left panel that the maximum magnitude of earthquakes that can occur on the sources affecting the hazard of L'Aquila is larger than M7. However, the rates of earthquakes larger than M6 are negligible compared with those of magnitude below M6. Conversely, it can be appreciated from the middle panel that if earthquakes with magnitude larger than M6 occur, for example, within 15 km from the site, the probability of exceeding $sa_{T_r = 475}$ is from 0.4 to almost 1 (ie, exceedance is almost certain for these scenarios). This, as extensively discussed in Iervolino et al,[6] shows why exceedance of the design spectra is expected in the epicentral areas of earthquakes of magnitude that would be considered relatively moderate otherwise, as systematically observed.[21]

3 | PEAK-OVER-THRESHOLD DISTRIBUTION

A consequence of the likely exceedance of the design actions in epicentral areas of moderate-to-high magnitude earthquakes is that structures will be exposed to actions larger than those considered in design. In other words, the design spectrum does not protect in the epicentral areas of these events. Therefore, it can be useful to quantify the expected GM in these earthquakes. To this aim, the expected POT was introduced in Iervolino et al [10] as the mean $Sa(T)$ conditional to the exceedance of the threshold corresponding to a return period of interest, indicated as sa_{T_r}. Following the common notation in probability, the expected POT can be indicated as $E[Sa(T)|Sa(T) > sa_{T_r}]$. It was demonstrated that it can be computed as:

$$E[Sa[T]|Sa[T] > sa_{T_r}] = \iint\limits_{M,R} e^{\mu_{Sa(T),m,r}} \cdot \int\limits_{\frac{\log(sa_{T_r}) - \mu_{Sa(T),m,r}}{\sigma_{Sa(T)}}}^{+\infty} e^{\sigma_{Sa(T)} \cdot z} \cdot f_{M,R,\varepsilon|Sa(T) > sa_{T_r}}(m,r,z) \cdot dz \cdot dr \cdot dm, \tag{5}$$

where all the terms and symbols have been already introduced, except $f_{M,R,\varepsilon|Sa(T) > sa_{T_r}}(m,r,z)$, which is the joint PDF of $\{M,R,\varepsilon\}$ given that $Sa(T) > sa_{T_r}$; ie, the *disaggregation* distribution for sa_{T_r}. (In this context, z denotes the generic realization of ε, and the lower limit of the inner integral is the ε value corresponding to the disaggregated acceleration value: $\left[\log(sa_{T_r}) - \mu_{Sa(T),m,r}\right]/\sigma_{Sa(T)}$.)

Note that Equation (5) is written assuming $\theta_{Sa(T)} = 0$ in the GMPE; however, the POT for any other value of $\theta_{Sa(T)}$ (eg, for any other soil condition) can be computed from Equation (5) as:

$$E\left[Sa(T)|Sa(T) > sa_{T_r}, \theta_{Sa(T)}\right] = e^{\theta_{Sa(T)}} \cdot E[Sa(T)|Sa(T) > sa_{T_r}]. \tag{6}$$

To link the POT to hazard disaggregation is functional to show that it has a negative correlation with ε; ie, at the sites where the average ε from disaggregation is lower, the POT is comparatively larger and vice-versa. In other words, where less anomalous GM is expected to cause exceedance, then the amount of exceedance is relatively larger and vice-versa.

Herein, a procedure to compute not only the expected value of the POT, but the full PDF of $Sa(T)$ given exceedance of sa_{T_r}, or $f_{Sa(T)|Sa(T) > sa_{T_r}}(sa)$, which does not require hazard disaggregation, is introduced. To start, the distribution of $Sa(T)$ in one generic earthquake,[†] $f_{Sa(T)}(sa)$, is needed. Such a distribution can be obtained from the absolute value derivative of the hazard curve divided by the total rate of earthquakes over the sources, $\nu = \sum_{i=1}^{s} \nu_i$:

$$f_{Sa(T)}(sa) \cdot d(sa) = \frac{1}{\nu} \cdot \left| \frac{d\lambda_{Sa(T) > sa}}{d(sa)} \right| \cdot d(sa) = \frac{1}{\nu} \cdot \left| d\lambda_{Sa(T) > sa} \right|. \tag{7}$$

At this point, the sought distribution, that is $f_{Sa(T)|Sa(T) > sa_{T_r}}(sa)$, it can be computed via the conditional probability rule:

───────────────────────────────────

[†]That is, given an earthquake of unknown magnitude and source-to-site distance.

$$f_{Sa(T)|Sa(T)>sa_{T_r}}(sa) = \frac{f_{Sa(T) \cap Sa(T)>sa_{T_r}}(sa)}{P[Sa(T)>sa_{T_r}]}, \tag{8}$$

where the denominator, $P[Sa(T)>sa_{T_r}]$ is the probability of exceeding the threshold in one generic earthquake and, in fact, is the rate of exceedance of sa_{T_r}, divided by the total rate of earthquakes:

$$P[Sa(T)>sa_{T_r}] = \frac{\lambda_{Sa(T)>sa_{T_r}}}{\nu}. \tag{9}$$

The numerator is the PDF of $Sa(T)$ when, at the same time, $Sa(T)>sa_{T_r}$. In other words, it is just the portion of $f_{Sa(T)}(sa)$ at the right of sa_{T_r}; then:

$$f_{Sa(T)|Sa(T)>sa_{T_r}}(sa) = \frac{f_{Sa(T)>sa_{T_r}}(sa)}{P[Sa(T)>sa_{T_r}]}. \tag{10}$$

Replacing Equation (7) in Equation (10), it results that the POT distribution is just the absolute value of the derivative of the hazard curve,[‡] truncated at the threshold and divided by the exceedance rate of threshold:

$$f_{Sa(T)|Sa(T)>sa_{T_r}}(sa) \cdot d(sa) = \frac{1}{\nu} \cdot \frac{|d\lambda_{Sa(T)>sa}|}{P[Sa(T)>sa_{T_r}]} = \frac{|d\lambda_{Sa(T)>sa}|}{\lambda_{Sa(T)>sa_{T_r}}}, \quad \forall sa > sa_{T_r}. \tag{11}$$

An example is given in Figure 3, where the POT distribution is derived for the 1-second spectral acceleration given the exceedance of the threshold with 475-year return period on rock in L'Aquila.

It follows that $E[Sa(T)|Sa(T)>sa_{T_r}]$, as well as any other statistical quantity, can just be computed from $f_{Sa(T)|Sa(T)>sa_{T_r}}$, in lieu of Equation (5). In this case, it is evident that the expected POT does not explicitly depend on the GMPE and hazard disaggregation, as it just requires the hazard curve. In other words, deriving the expected POT from the POT distribution results in a procedure simpler than Equation (5). Moreover, this procedure also allows to easily retrieve the spectrum of the peak-over-the-thresholds (as it will be clear in Section 5) given the exceedance of sa corresponding to any return period.[§]

Finally, it is noted that the term *peak-over-threshold* is somewhat common in time-variant reliability problems[22]; however, its definition herein is closer to the concept of *superquantile* or *conditional quantile* from risk analysis.[23]

4 | POT DISTRIBUTIONS AND SITE'S HAZARD

In this section, the distribution of the spectral acceleration given the exceedance of some threshold values is discussed for Milan, Naples, and L'Aquila. The objective is to discuss the effect of the site's hazard on the shape of the POT distribution, varying the return period of the threshold and the spectral ordinate of interest. To this aim, for the three considered sites, the POT distribution for PGA and $Sa(T = 1s)$ were computed as discussed in the previous section. The thresholds are those that have exceedance return period equal 50, 475, and 2475 years, according to the hazard curves of Figure 1. The first two return periods have been chosen because they correspond to the *damage* and *life-safety* limit states of an ordinary structure according to the Italian building code, respectively, while $T_r = 2475yr$ is the maximum return period considered by the code. Therefore, six distributions are computed for each site and displayed in Figure 4.

[‡]It follows that the POT's complementary cumulative distribution function is just $P[Sa(T)>sa|Sa(T)>sa_{T_r}] = 1$ for $sa \leq sa_{T_r}$, and $P[Sa(T)>sa|Sa(T)>sa_{T_r}] = \lambda_{Sa(T)>sa}/\lambda_{Sa(T)>sa_{T_r}}$, for $sa > sa_{T_r}$, that is, the normalized tail of the hazard curve.

[§]Although it could also be done via Equation (5), it would require disaggregation to be performed for all the return periods of interest. However, it is to note that Equation (5) can be more robust computationally, because Equation (11), to produce unbiased results, requires the hazard curve be computed up to sa values sufficiently large so that the area under the PDF equals one.
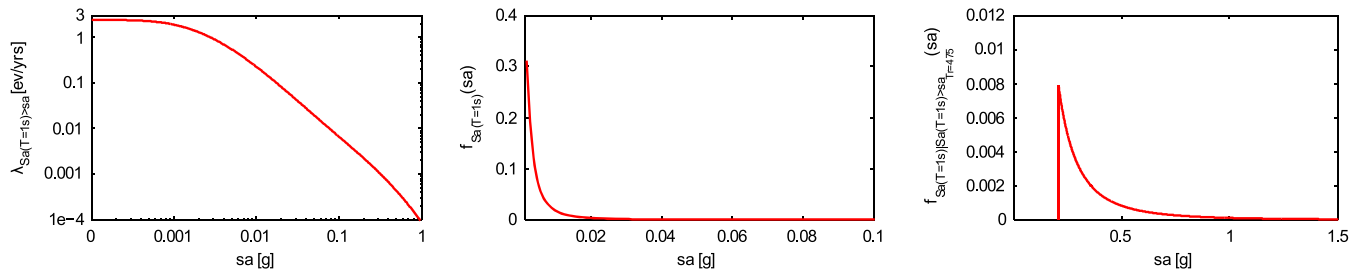
FIGURE 3 Left: 1-second spectral acceleration hazard curve for the site of L'Aquila; center: distribution of 1-second spectral acceleration in one earthquake; right: POT distribution relative to exceedance of the spectral acceleration with 475-year exceedance return period from the left panel [Colour figure can be viewed at wileyonlinelibrary.com]
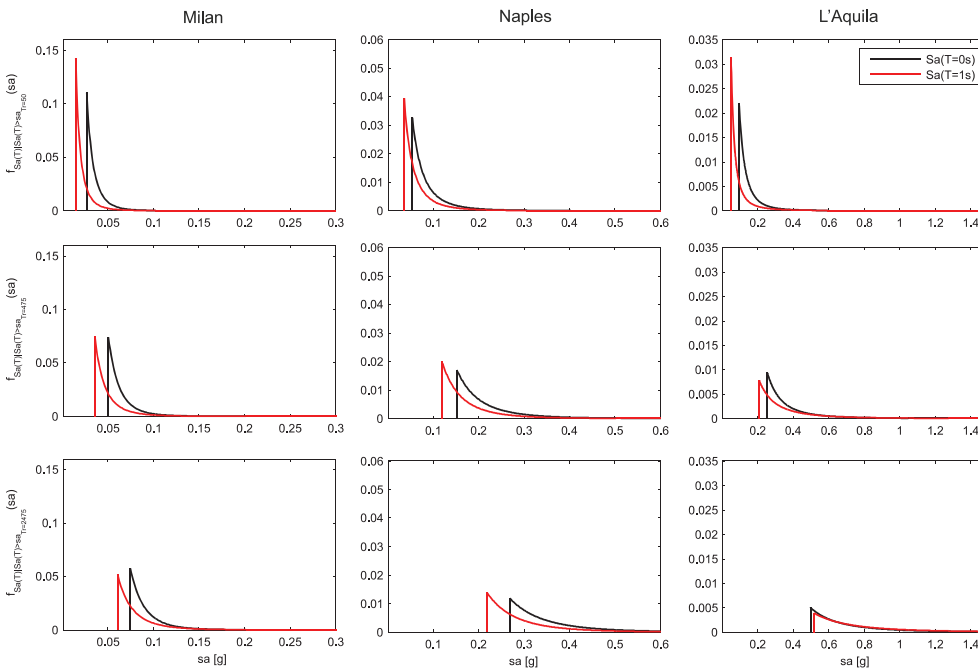

FIGURE 4 POT distributions of PGA and 1-second spectral acceleration conditional on the exceedance of the threshold with return period equal to: 50 (top), 475 (middle), and 2475 years (bottom) [Colour figure can be viewed at wileyonlinelibrary.com]

Looking at the figure horizontally, that is the same return period for different sites, it is shown that the POT distribution tends to get wider (ie, the POT random variable is comparatively more *dispersed*) as the hazard for the site increases. This result applies to both the spectral ordinates considered. Given the discussion of Section 3, the explanation is in the shape of the hazard curves. As it can be seen from Figure 1, the larger the hazard the lower the (negative) slope of the hazard curve at the threshold (see also Section 7.1). Exploring the figure vertically, that is, different return periods for the same site, it appears that also in this case the POT distribution gets flatter. This is less obvious as, heuristically, one could think that the larger the threshold the lower the peak over it. In fact, the expected value of the POT should asymptotically tend to the threshold; however, the heterogeneity of spectral acceleration given exceedance tends to get wider (to follow).

As a summary, Table 1 reports the thresholds, the expected values, the standard deviations, the coefficients of variation (CoV) of the POT distributions, and the absolute values of hazard curve slope's (h) at the threshold, in log-log scale, for the three sites. As discussed, both the standard deviation and the CoV of the POT are larger for the most hazardous sites. In other words, the larger the hazard of the site, the more uncertain (also relatively to the mean) the spectral acceleration given exceedance is. Moreover, for any site, one can see that, invariably, increasing the return period of exceedance of the threshold, the standard deviation increases; however, the CoV decreases, although mildly. In other words, the larger the hazard of the site and/or the return period of the threshold the more uncertain the spectral acceleration given exceedance is; however, it is decreasing if measured relatively to the mean.

The table also reports the 95th percentile from the POT distribution ($sa_{95\%}$), which will be discussed more thoroughly later. It has been chosen as a measure of how large the POT can be at a specific site. It can also be interpreted as

TABLE 1 Mean, standard deviation, CoV, 95th percentile of POT distributions, and slope of the hazard curve at the threshold, from Figure 4

		MI		NA		AQ	
		$Sa(T=0s)$	$Sa(T=1s)$	$Sa(T=0s)$	$Sa(T=1s)$	$Sa(T=0s)$	$Sa(T=1s)$
$T_r = 50yr$	sa_{T_r} [g]	0.026	0.014	0.054	0.036	0.094	0.049
	h	3.093	2.192	1.810	1.470	2.099	1.575
	Expected POT [g]	0.036	0.023	0.096	0.072	0.165	0.119
	St. dev. [g]	0.013	0.013	0.058	0.049	0.118	0.147
	CoV	0.350	0.556	0.600	0.691	0.712	1.237
	$sa_{95\%}$ [g]	0.059	0.045	0.198	0.158	0.345	0.318
$T_r = 475yr$	sa_{T_r} [g]	0.050	0.035	0.152	0.119	0.253	0.207
	h	3.866	2.745	2.618	2.414	2.398	1.637
	Expected POT [g]	0.065	0.052	0.225	0.182	0.412	0.412
	St. dev. [g]	0.018	0.021	0.091	0.080	0.225	0.316
	CoV	0.277	0.413	0.405	0.441	0.545	0.766
	$sa_{95\%}$ [g]	0.099	0.090	0.394	0.327	0.817	0.937
$T_r = 2475yr$	sa_{T_r} [g]	0.074	0.060	0.268	0.218	0.496	0.515
	h	4.440	3.228	3.226	3.063	2.532	2.043
	Expected POT [g]	0.093	0.083	0.368	0.306	0.753	0.868
	St. dev. [g]	0.023	0.029	0.120	0.108	0.319	0.486
	CoV	0.242	0.345	0.325	0.354	0.424	0.559
	$sa_{95\%}$ [g]	0.136	0.135	0.593	0.504	1.353	1.723

the value of spectral acceleration to be expected one-in-twenty earthquakes causing exceedance of the threshold of interest (in fact, it represents the GM that corresponds to a return period equal to that of the threshold divided by 1-0.95; ie, in the case of the threshold with $T_r = 475yr$, the 95th POT percentile is $sa_{95\%} = sa_{T_r=9500}$).

As it regards the slope, it is increasing with the return period, as expected, and generally decreasing with site's hazard, although not always.

Considering the site of L'Aquila (right panels of Figure 4), which is in the central Italy Apennines, one of the most seismically hazardous areas in the country, the POT distribution for PGA is over the intervals (0.094g; +∞) and (0.253g; +∞) for the return periods of $T_r = 50yr$ and $T_r = 475yr$, respectively (obviously, the lower ends of the intervals are the thresholds with the considered exceedance return period). The 95th percentile of the spectral acceleration is 0.345 g for $T_r = 50yr$, which means that one-in-twenty earthquakes exceeding the PGA with 50 years return period are expected to almost double the acceleration with 475-year return period at the site. In L'Aquila, the expected value of the POT is 0.75 g for the threshold with $T_r = 2475yr$, while the 95th POT percentile is as high as 1.35 g. A similar reasoning applies to the 1-second spectral ordinate; however, the relative difference between the expected value and the threshold, as well as between the 95th percentile and the threshold, is larger for $Sa(T = 1s)$ than PGA, for each return period.

In the case of Naples (middle panels of Figure 4), which is exposed to generally lower seismic hazard with respect to L'Aquila, it can be observed that, with reference to $Sa(T = 1s)$, the PDF of the acceleration conditional on the exceedance of the threshold with $T_r = 50yr$ is defined for values larger than 0.036 g, while it is defined over the interval (0.119g; +∞) for $T_r = 475yr$, and (0.218g; +∞) for $T_r = 2475yr$. The values of the 95th POT percentile, still in terms of $Sa(T = 1s)$, if the exceedance of the corresponding ordinate of the UHS with $T_r = 50yr$ and $T_r = 475yr$ occurs, are 0.158 and 0.327 g, respectively. For $T_r = 2475yr$, the 95th POT percentile is about 0.5 g.

It is also worthwhile to consider the case of Milan that, unlike the other two sites, is outside the seismic sources of the model considered for the hazard analysis (see Figure 1). In fact, the conditional PDF of the considered spectral accelerations (left panels of Figure 4) are informative about what to observe for code-conforming structures located in the low-hazard regions in the case exceedance of the design spectrum occurs. Looking at the distribution of $Sa(T = 1s)$ for the threshold with $T_r = 50yr$, which is defined over the interval (0.014g; +∞), one can observe that the 95th percentile is equal to 0.045 g, which is more than three times the corresponding ordinate of the spectrum. Looking at the

larger return periods, the domain of the distribution for $Sa(T = 1s)$ reduces to $(0.035g; +\infty)$ for $T_r = 475yr$ and to $(0.060g; +\infty)$ for $T_r = 2475yr$; the 95th percentiles of the spectral ordinate over the threshold are equal to about 0.1 and 0.135 g, respectively.

To extend the results discussed so far to a larger number of return periods, 30, 50, 70, 100, 140, 200, 475, 975, and 2475 years, are considered. For these return periods, Figure 5 provides the percentage difference of the POT for the three sites and the two spectral ordinates. These differences are defined as $\Delta^\% = 100 \cdot \{E[Sa(T)|Sa(T) > sa_{T_r}] - sa_{T_r}\}/sa_{T_r}$ and $\Delta^\% = 100 \cdot [sa_{95\%} - sa_{T_r}]/sa_{T_r}$ for the expected POT and the 95th percentile, respectively. The most important result the curves show is that, generally, the percentage increment is not uniform across the sites, even for the same return period of the threshold. Moreover, the increment tends to decrease as the return period increases, as expected, however, relatively mildly.

With reference to L'Aquila, once the exceedance of the design PGA with $T_r = 2475yr$ occurs, one can observe that such exceedance is expected to be equal to 52%, and there is 5% probability that the difference is larger than 172%. Coherently with the results obtained at a national scale (to follow), the curves in Figure 5 show that percentage differences are smaller for PGA than $Sa(T = 1s)$. In fact, for the latter spectral ordinate, the minimum value of the increase in the expected POT, in the investigated range of return periods, is equal to 68%, and it results equal to 234% for the 95th percentile.

For the case of Milan, even if the design threshold is exceeded due to a more *anomalous* ground motion,[¶] the relative amount of exceedance is smaller than in L'Aquila.[10] In fact, for the PGA, the percentage increments of the expected value and 95th percentile of the acceleration beyond the threshold with $T_r = 2475yr$, are equal 26% and 83%, respectively. With reference to $Sa(T = 1s)$, the minimum percentage difference of the expected exceedance, in the investigated range of return periods, is equal to 38%, and it is 125% for the 95th percentile.

The case of Naples generally shows intermediate values with respect to the other two sites considered, confirming that the hazard level has a positive correlation with the POT in both absolute and relative terms. In fact, the relevant result here is that the GM, in case of exceedance of the design spectra with the same return period, is significantly larger for sites exposed to comparatively larger hazard (eg, twice in L'Aquila with respect to Milan) and although this can now seem intuitive, it is not accounted for in current performance-based seismic design and can have an effect of seismic safety implied in code-conforming design, as discussed in Section 6.

5 | SPECTRA-OVER-THRESHOLD

Because seismic design actions are represented in the form of spectra, it would be beneficial to compare with the POT represented in terms of spectra as well. To this aim, it is possible, for each spectral ordinate in a range of natural vibration periods and for a given return period of exceedance at a site, to plot the expected value of the POT versus the vibration period. The resulting spectrum collects the expected spectral accelerations conditional to the exceedance of the corresponding UHS ordinates. In a similar manner, if a specific percentile of the POT distribution is selected, it is possible to build the spectrum collecting the POT ordinates corresponding to the same percentile. These functions can be referred to as *uniform-POT* spectra. In Figures 6, 7, and 8, the uniform-POT spectra are provided for the three sites and return periods considered in Section 4. In fact, in the figures, the corresponding UHS are also given, along with the spectra for: (a) the expected value and (b) the one-in-twenty value of the accelerations given the exceedance of the corresponding ordinate in the UHS; ie, the 95th POT percentile spectra. (All spectra are lumped at the natural vibration periods considered by the adopted GMPE.)[16] Moreover, in each figure, the middle and right panels provide the absolute and relative differences of the two POT spectra with respect to the corresponding UHS. The relative differences have been already defined in the previous section, while the absolute differences are $\Delta = E[Sa(T)|Sa(T) > sa_{T_r}] - sa_{T_r}$ and $\Delta = sa_{95\%} - sa_{T_r}$ for the expected POT and its 95th percentile, respectively.

It can be preliminarily observed that, as expected, the shape of the spectra-over-the-thresholds is not different from that of the UHS. This is because the conditional PDFs of the different spectral accelerations only depend on the hazard curves; indeed, similarly to the latter, they vary with the natural vibration period according to the considered GMPE. Furthermore, while the percentage increments decrease with the return period for almost all the spectral ordinates, the opposite trend can be found for the absolute differences.

[¶]The expected value of ϵ, for any given return period, is systematically larger in Milan rather than in L'Aquila.[11]

FIGURE 5 Percentage difference of expected value (top) and 95th percentile (bottom) of the spectral accelerations with respect to the corresponding threshold, as a function of its return period of exceedance
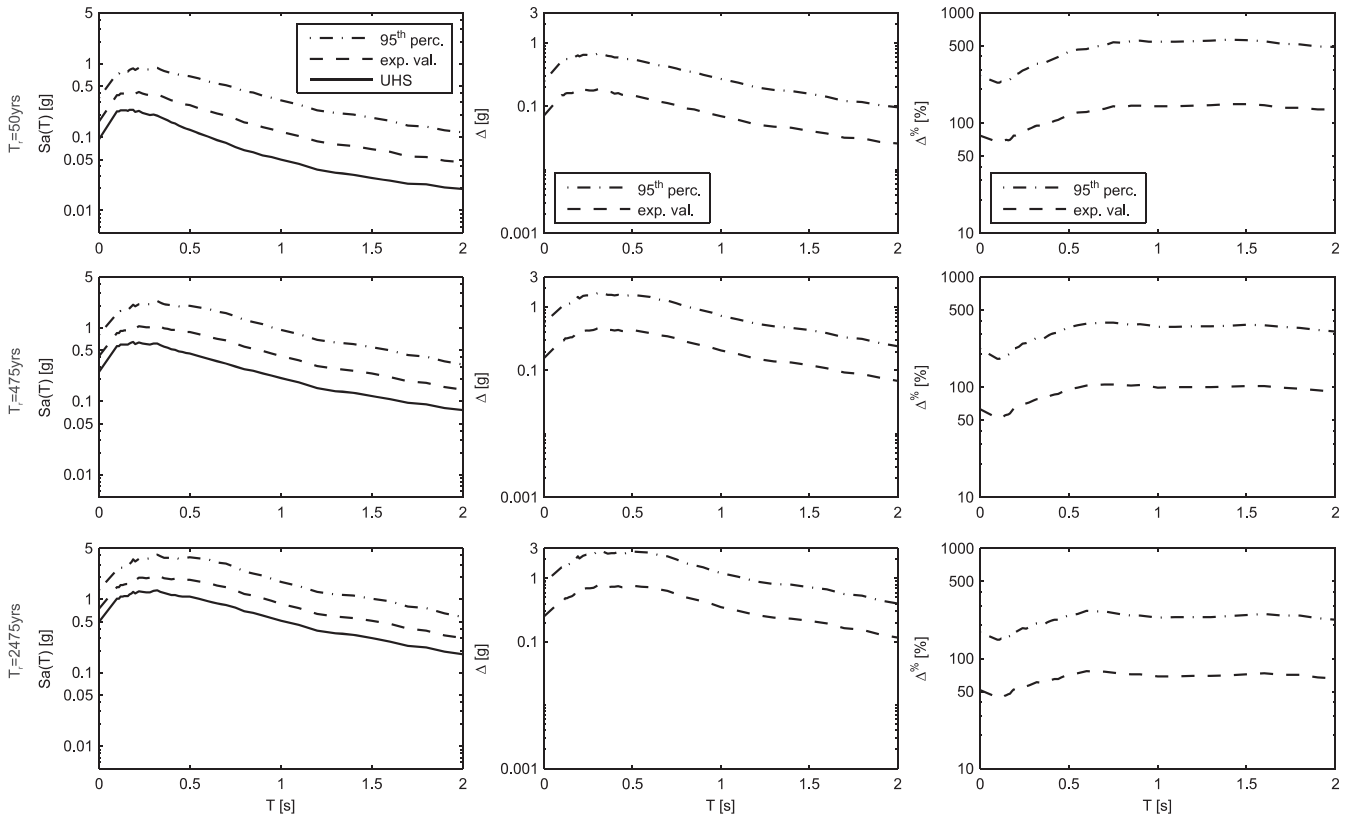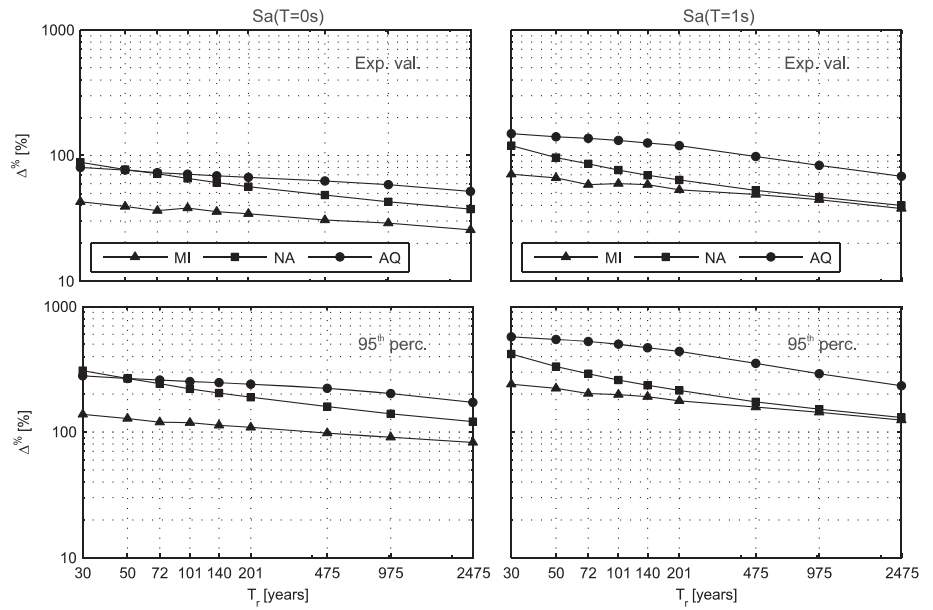

FIGURE 6 Expected and 95th percentile POT spectra and UHS for 50 (top), 475 (middle), and 2475 (bottom) years return period in L'Aquila (left); for each return period, absolute (center) and percentage (right) differences with the exceeded UHS are also provided

To further analyze these figures, it could be useful to discuss the sites individually. For L'Aquila (Figure 6), the percentage increments of the expected POT spectrum with respect to the design thresholds are up to 150%, 106%, and 80% in the case the exceedance of the UHS with 50, 475, and 2475-year return periods, respectively; they occur at vibration periods equal to 1.4, 0.75, and 0.6 seconds, respectively. The maximum absolute differences for the expected POT spectrum are equal to 0.2, 0.5, and 0.8 g for 50, 475, and 2475 years, and all occur at a vibration period equal to 0.32 second. For what concerns the 95th percentile spectrum, considering, for example, 475 years as the return period, the maximum is about 2.3 g and occurs at 0.32 second.
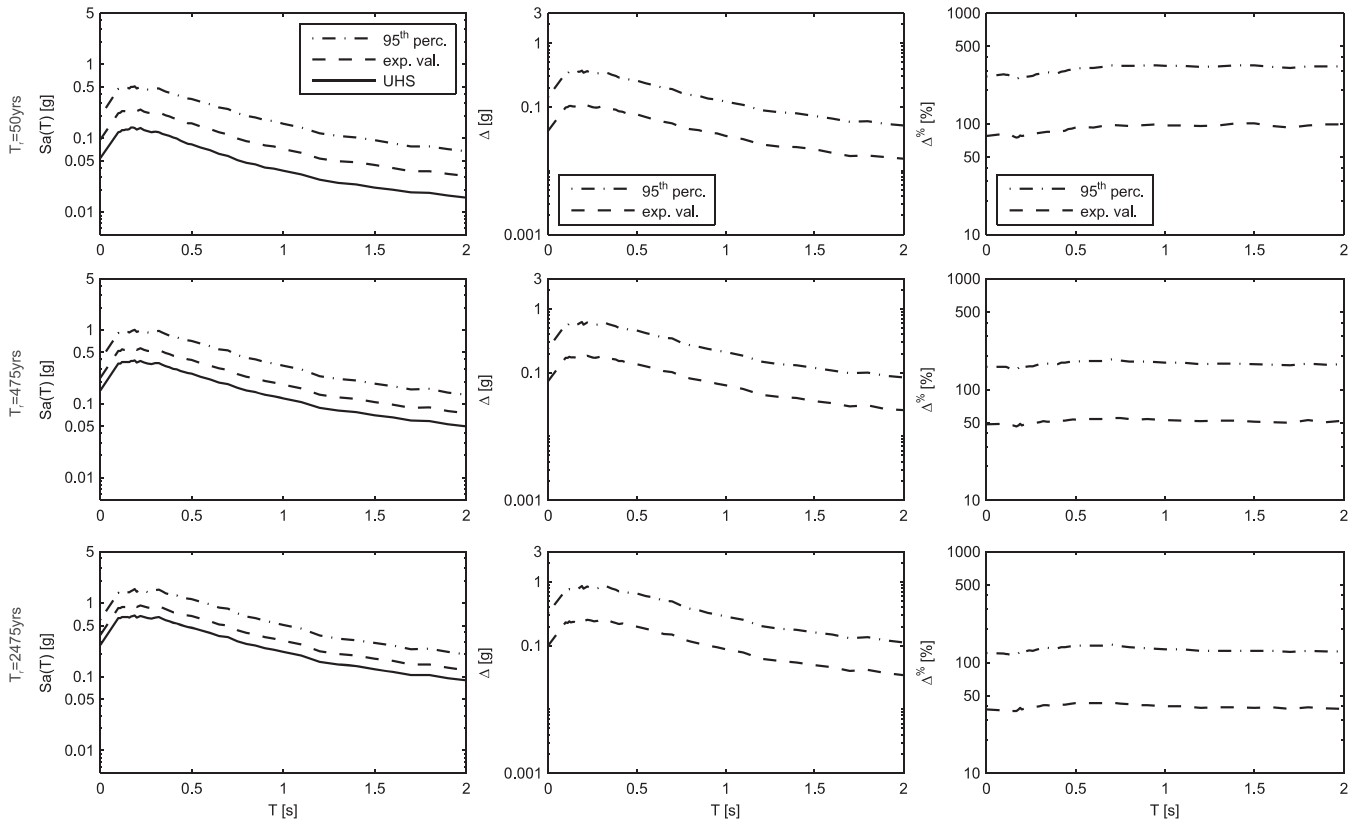
FIGURE 7 Expected and 95th percentile POT spectra and UHS for 50 (top), 475 (middle), and 2475 (bottom) years return period in Naples (left); for each return period, absolute (center) and percentage (right) differences with the exceeded UHS are also provided
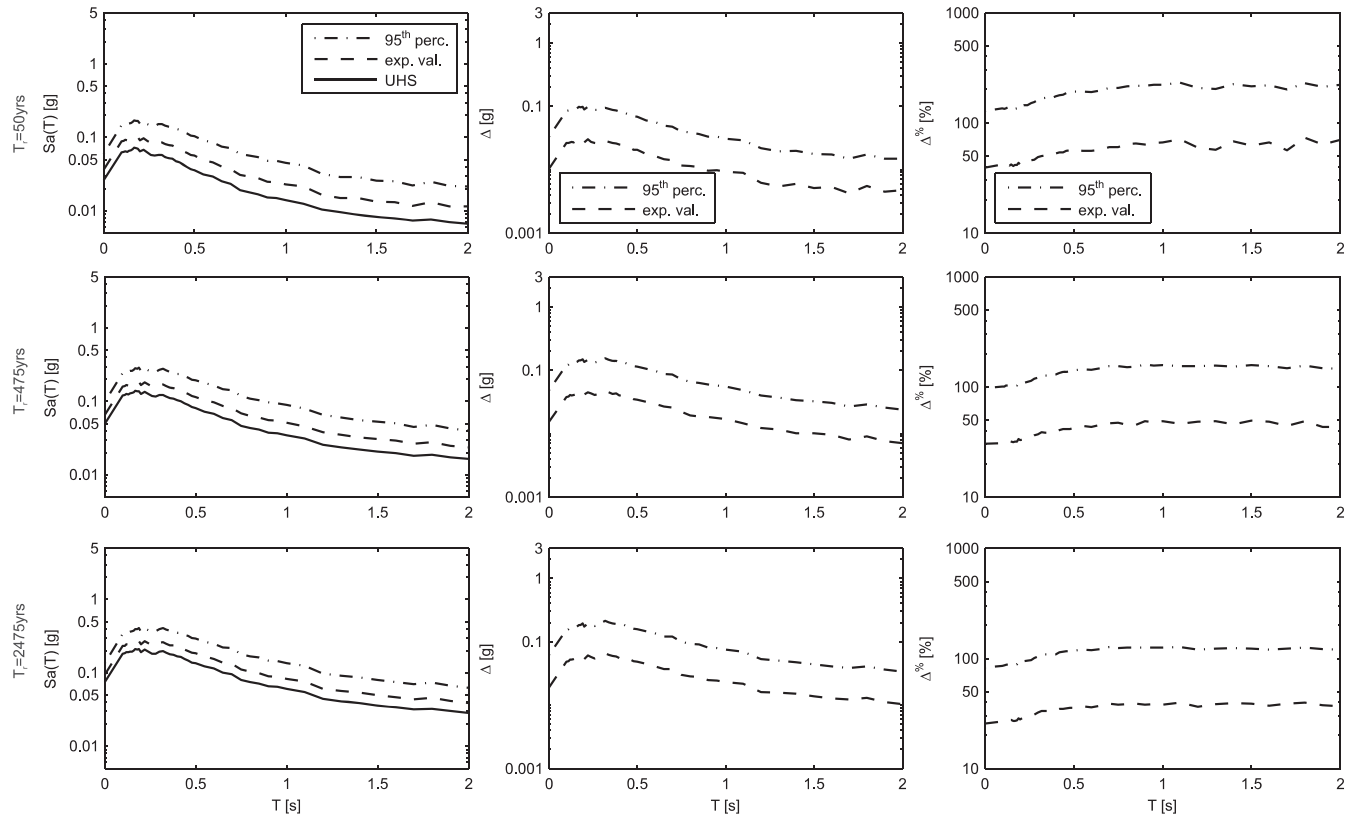

FIGURE 8 Expected and 95th percentile POT spectra and UHS for 50 (top), 475 (middle), and 2475 (bottom) years return period in Milan (left); for each return period, absolute (center) and percentage (right) differences with the exceeded UHS are also provided

With reference to Naples (Figure 7), the ordinates of both POT spectra are always smaller than in L'Aquila, consistent with the results of the previous section. In fact, for the expected POT spectrum, the maximum percentage increments are equal to 100%, 55%, and 43% for the considered return periods in ascending order. The maxima occur at $T = 1.40s$ for $T_r = 50yr$ and at $T = 0.70s$ for both $T_r = 475yr$, and $T_r = 2475yr$. The maximum absolute differences are equal to 0.11, 0.19, and 0.26 g for the three (increasing) return periods; these maxima occur at $T = 0.19s$ for $T_r = 50yr$ and $T_r = 475yr$, and at $T = 0.32s$ for $T_r = 2475yr$. Looking at the spectrum of the 95th percentile of the POT for $T_r = 475yr$, it can be seen that the maximum is around 1 g, occurring at $T = 0.19s$

In the case of Milan (Figure 8), the percentage increments of the expected POT spectrum with respect to the design thresholds are up to 73%, 50%, and 40%, in the case the exceedance of the thresholds with 50, 475, and 2475 years return period, respectively. They occur at vibration periods equal to 1.8, 1.5, and 1.8 seconds, respectively. The maximum absolute difference of the expected POT spectrum, in ascending order of the return period, are equal to 0.03, 0.05, and 0.065 g and occur at $T = 0.17s$ for $T_r = 50yr$, and at $T = 0.32s$, for the other two return periods. With reference to the 95th POT spectrum corresponding to $T_r = 475yr$, the maximum value is slightly smaller than 0.3 g and occurs at $T = 0.19s$.

As a conclusion, the spectra of the peak-over-the-threshold show that, in case of exceedance (eg, when the site is in the epicentral area of a moderate-to-high magnitude earthquake), the largest absolute differences with the considered threshold are observed at the low-to-mid vibration periods. The vibration periods corresponding to the maxima tend to decrease with the increasing return period. The maximum percentage increments tend to occur at lower vibration and return periods; however, they show less sensitivity to the vibration period than the return period of the considered threshold.

5.1 | Conditional POT spectrum

Finally, it is noted that the definition of the POT spectra given in this section does not contemplate any stochastic dependency between spectral ordinates, which are known to exist in one earthquake. This is for consistency with the UHS to which the POT spectra are compared. Nevertheless, it is worth noting that POT spectra can be computed in analogy with other forms of spectra, which account for correlation of spectral ordinates, such as the conditional mean spectrum (CMS).[24,25] In particular, once a spectral ordinate at a vibration period of interest (T^*) is chosen and the expected POT is computed, then the other spectral ordinates can be obtained as:

$$
E\{\log[Sa(T)]\} = \iint_{M,R} \left\{ \mu_{Sa(T),m,r} + \rho_{T,T^*} \cdot \sigma_{Sa(T)} \cdot \frac{E\left[Sa(T^*)|Sa(T^*)>sa_{T_r}\right] - \mu_{Sa(T^*),m,r}}{\sigma_{Sa(T^*)}} \right\} \cdot f_{M,R|Sa(T^*)=E\left[Sa(T^*)|Sa(T^*)>sa_{T_r}\right]}(m,r) \cdot dr \cdot dm, \quad (12)
$$

where, as already introduced, sa_{T_r} is the value with T_r exceedance return period of the spectral acceleration at the vibration period T^*. All the terms in the equation have been defined already, except $f_{M,R|Sa(T^*)=E\left[Sa(T^*)|Sa(T^*)>sa_{T_r}\right]}$, which is the magnitude-distance disaggregation distribution given the expected POT, and ρ_{T,T^*}, which is the correlation coefficient of the spectral accelerations at the two periods $\{T,T^*\}$. The equation allows, analogously, to compute the CMS spectra corresponding to any other POT percentile.
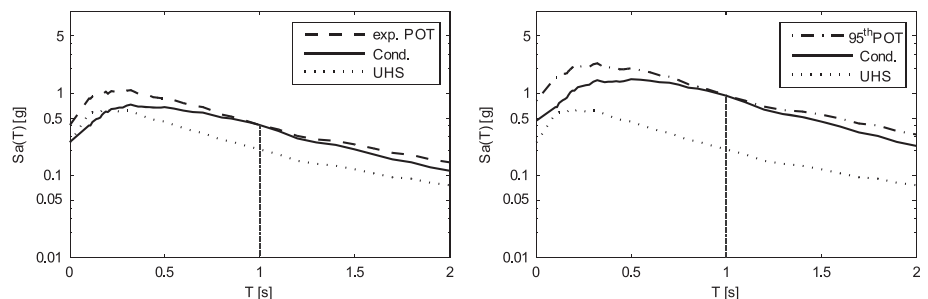

FIGURE 9 CMS conditional to the expected value (left) and 95th percentile (right) POT for the 1-s spectral acceleration with 475-year return period in L'Aquila

TABLE 2 Failure rates and strength reduction factors for six-story reinforced concrete code-conforming structures. (*The rate was so low that only an upper bound could be provided; see Iervolino et al [9] for details)

	MI	NA	AQ
Global collapse annual failure rate	1.00E − 5*	1.00E − 5*	8.47E − 5
Usability-preventing damage annual failure rate	1.86E − 4	5.97E − 3	1.08E − 2
$R_{POT} = E\left[Sa\left(T^*\right)\middle|Sa\left(T^*\right) > sa_{T_r=475}\right]/sa_y$	0.41	1.16	2.19
$R_{UHS} = sa_{T_r=475}/sa_y$	0.28	0.77	1.10

As an example, Figure 9 provides the POT-CMS for the site of L'Aquila, given the exceedance of 1-second spectral acceleration from the 475 years UHS (computed with the correlation model by Baker and Jayaram).[26] In particular, the left panel shows the UHS, the expected value of the POT (ie, the same as in Figure 6), and the conditional spectrum computed according Equation (12). The right panel shows the conditional spectra corresponding to the 95th percentile of the POT for the same spectral ordinates, as well as the 95th percentile POT spectrum, and the UHS from Figure 6.

6 | PEAK-OVER-THRESHOLD AND SEISMIC RELIABILITY OF CODE-CONFORMING STRUCTURES

In this section, it is discussed how the POT can help understanding the seismic structural safety of code conforming structures. To this aim, some structures designed, modeled, and analyzed in the RINTC research project[27] are considered. The project evaluated the seismic structural reliability (ie, the *annual failure rate*) of structures, belonging to several structural typologies and designed for different seismic hazard levels across the country. In particular, the same sites (ie, Milan, Naples, and L'Aquila) of this study were considered.

The structures have been designed with respect to two limit states, that is, *damage* and *life-safety*. The design GM has return period of 50 years for the former and 475 years for the latter. In turn, in the project, the annual failure rates have been evaluated with respect to two performances named *usability-preventing damage* (UPD) and *global collapse* (GC). Failure with respect to UPD is related to damage to nonstructural elements (eg, infills in reinforced-concrete buildings), while GC is related to the loss of lateral strength of the structural system.

One of the main results of the project is that the seismic structural reliability of code-conforming structures tends to decrease as the hazard of the site increases, despite the exceedance return period of the design GM being the same at all sites.[9] As an example of such a result, the failure rates of the six-story (bare) moment-resisting frames from the RINTC project are given in Table 2, where it can be seen that they grow by orders of magnitude as the hazard of the site increases. One of the explanations for these results could possibly be related to issues that can be grossly categorized as the *design minima*; ie, the requirements that the code imposes regardless of the design seismic actions and that are expected to have a larger effect on the seismic safety of structures designed for low-hazard sites (for structural design and modeling details, see Ricci et al).[28] However, as it is discussed here, the GM beyond that considered for design can also play a role with respect to this issue.

Figure 10 (top) shows the equivalent single-degree-of-freedom system backbones for the considered structures (ie, six-story [bare] moment-resisting frames) designed at the three sites, which are obtained from the original three-dimensional structural models as discussed in Suzuki et al.[29] It can be seen that, as expected, the maximum strength and displacement (Sd) capacity of code-conforming structures increase as the hazard of the site increases. These backbones are rendered nondimensional, thus more easily comparable, in Figure 10 (bottom), where the coordinates are the displacement ductility (μ) and the strength reduction factor (R). On the same figure, the 475-year UHS for the sites (ie, approximately that used for design), as well as the expected POT spectra, are also shown in the acceleration-displacement format. (Spectra are not exactly those of the previous section because structural design of the considered structures refers to soil site class C according to EC8.)[2]

At Milan, the UHS demand is in the elastic range, and a hypotethical *performance point*, according to Fajfar,[30] would move to the right of the backbone as the seismic hazard increases. This can be considered the effect of the code requirements discussed earlier. However, in the figure, the expected POT spectra are also shown for the three sites. The

FIGURE 10 Top: equivalent single-degree-of-freedom system backbones for six-story reinforced-concrete code-conforming structures; bottom: acceleration-displacement spectra and performance points in normalized (ie, strength reduction factor vs ductility) format
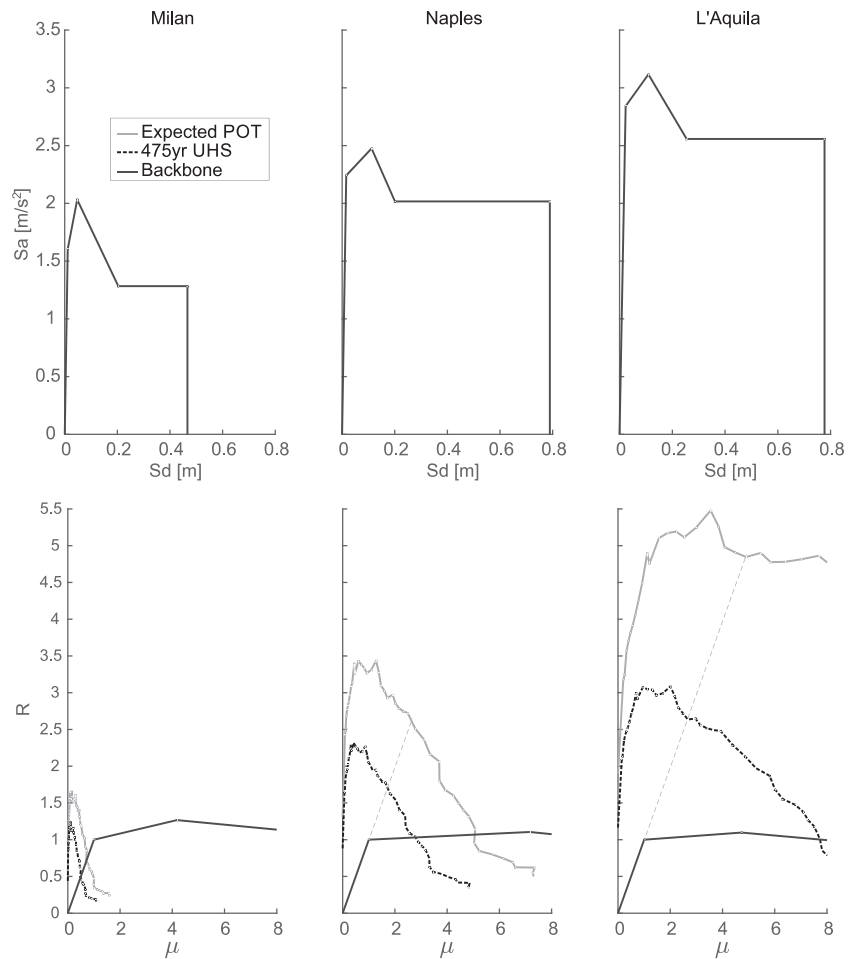
seismic demands according to these spectra also change as the hazard of the site increases; however, it happens in a disproportionate way with respect to what happens for the UHS, and this can have a non-negligible impact on the seismic structural reliability. To quantify this effect, Table 2 provides the strength reduction factors computed with respect to the expected POT (R_{POT}) and the UHS (R_{UHS}). These factors are defined as the values from the respective spectra, at the period of the considered system, divided by the yielding spectral acceleration (sa_y) of the system. It is easy to note a larger increase, with site's hazard, of the R_{POT} with respect R_{UHS}.

It can be concluded that the GM exceeding the design one, for which the structure is not verified during design, is significantly different at the three sites, so that it has an effect on seismic structural safety even if the design GM has the same return period across the sites, and the worst situation is for the sites exposed to the larger hazard. One solution to this issue is, in principle, the design based on risk-targeted GMs, which overcomes the return period approach discussed herein and provides a given degree of structural safety assuming a reference fragility function for the structure being designed. However, the paradigm according to which design explicitly targets a certain level of structural safety has not found yet its way fully in many codes worldwide, one significant example being the EC8 and similar building codes as the Italian one, which are and will be for quite some time still based on static and modal analyses via *behavior* (ie, strength reduction) factors. To account for the issues brought by the POT in this framework, there are at least two possible remedies that are currently under preliminary discussion in the scientific community. A straightforward one would be to calibrate behavior factors so that they are hazard and POT dependent; ie, in a reverse manner as addressed in the illustrative structural application of this section, so that to achieve a comparable structural safety of the structures designed at different sites (see also the work of Suzuki,[31] for a more comprehensive assessment of the strength reduction factors for a variety of code-conforming structural typologies). Alternatively, it could be argued that for structures located in sites where the POT is larger, the design action is possibly largely exceeded when the site is the epicentral area of a moderate-to-high earthquake. Therefore, an additional performance objective could be verified for the

structures designed in these sites. The seismic action for this further limit state should be derived from the POT distribution. In other words, referring for example to the EC8 limit states: a structure designed for life-safety, should also be verified for *collapse-prevention* when the GMs equal the expected POT. However, any code-ready proposal requires further research work.

7 | POT PERCENTILE MAPS

This section is intended, with reference to Italy, to provide insights on the POT range of variability, when different return periods are considered, at a national scale, considering the same hazard model recalled in Section 2. [#] In particular, these maps were carried out considering $sa_{T_r=50}$, $sa_{T_r=475}$, and $sa_{T_r=2475}$ as the reference thresholds. Results are shown in Figures 11 and 12 for PGA and $Sa(T=1s)$, respectively. In particular, the top, middle, and bottom panels refer to $T_r=50yr$, $T_r=475yr$, and $T_r=2475yr$, respectively. For a given return period, the maps show, from left to right, the thresholds according to the considered hazard model, the expected value, and the 95th percentile from the POT distributions at each site, as discussed in Section 3. For each map and in both figures, the location where the maximum for each map occurs and areal source zones adopted in the analyses are also provided.

The figures show that the design thresholds are larger along the central-southern Apennines mountain chain and in the Calabrian arch, regardless of the return period of interest. Considering $T_r=2475yr$, the largest value of the threshold across Italy is around 0.6 g for both the spectral ordinates.

As expected from the analysis of the three sites above, the larger is the threshold at the site, the larger are the expected value and the 95th percentile of the spectral acceleration given exceedance. This is also true when, for a given site, the statistics of the POT, at different return periods, are considered. In fact, looking at the figures vertically, it can be noted that both the expected POT and $sa_{95\%}$ increase with the return period at all the sites. Given the exceedance of $sa_{T_r=2475}$, the maximum value of the expected acceleration across Italy is around 1 g for both the spectral ordinates, while the maximum value of $sa_{95\%}$ is 1.5 g in the case of PGA and even a little above 2 g for $Sa(T=1s)$.

The relative difference between the statistics of the POT and the threshold from the data are also larger in the most hazardous areas. These differences tend to decrease with the increasing return period, although mildly. For example, with reference to PGA, the expected POT can be as high as two times the threshold when the exceedance of $sa_{T_r=50}$ occurs in some areas along the southern Apennines mountain chain. On the other hand, considering the same areas, if the exceedance of the $T_r=2475yr$ PGA is of interest, the acceleration over the threshold is expected to be equal around 1.5 times the threshold. These results are also consistent with what discussed for the three sites in Section 4.

On average, the percentage differences, over the country, of the expected peak over threshold with 50-year return period, are equal to 67% and 104% for PGA and $Sa(T=1s)$, respectively. In the case $T_r=475yr$, the differences are equal to 50% for PGA and 70% for $Sa(T=1s)$. When $T_r=2475yr$, the amount of exceedance of the threshold is equal to 41% in the case of PGA and 54% in the case of $Sa(T=1s)$. In the case of $sa_{95\%}$, the average percentage difference is equal to 233% for PGA and 375% for $Sa(T=1s)$, when the exceedance of $sa_{T_r=50}$ is of interest. Like the expected POT, these differences tend to decrease with the return period. In fact, for PGA, they are equal to 170% and 134% for $T_r=475yr$ and $T_r=2475yr$, respectively, and 243% and 183% for $Sa(T=1s)$. However, the figures confirm that the amount of exceedance over the threshold strongly varies from site-to-site depending on the site's hazard.

7.1 | POT vs hazard curve's slope

Note that the absolute value of the local slope of the hazard curve at the threshold, which—as discussed by McGuire[12]—is related to the structural reliability, can be considered a proxy for the POT. In fact, $10^{1/h}$ represents the

---

[#]In fact, the expected value of the acceleration over the design threshold with 475 years was already mapped for Italy.[10] That analysis was helpful in showing that when ε is large, the expected value of POT is low and vice-versa. It was found that, when an anomalous ground motion is required to cause exceedance, the expected amount of exceedance is comparatively low with respect to those location where exceedance is due to a less anomalous ground motion (ie, lower ε). Because the hazard disaggregation generally shows smaller ε in high-hazard sites, it means that in these areas the exceedance is larger.
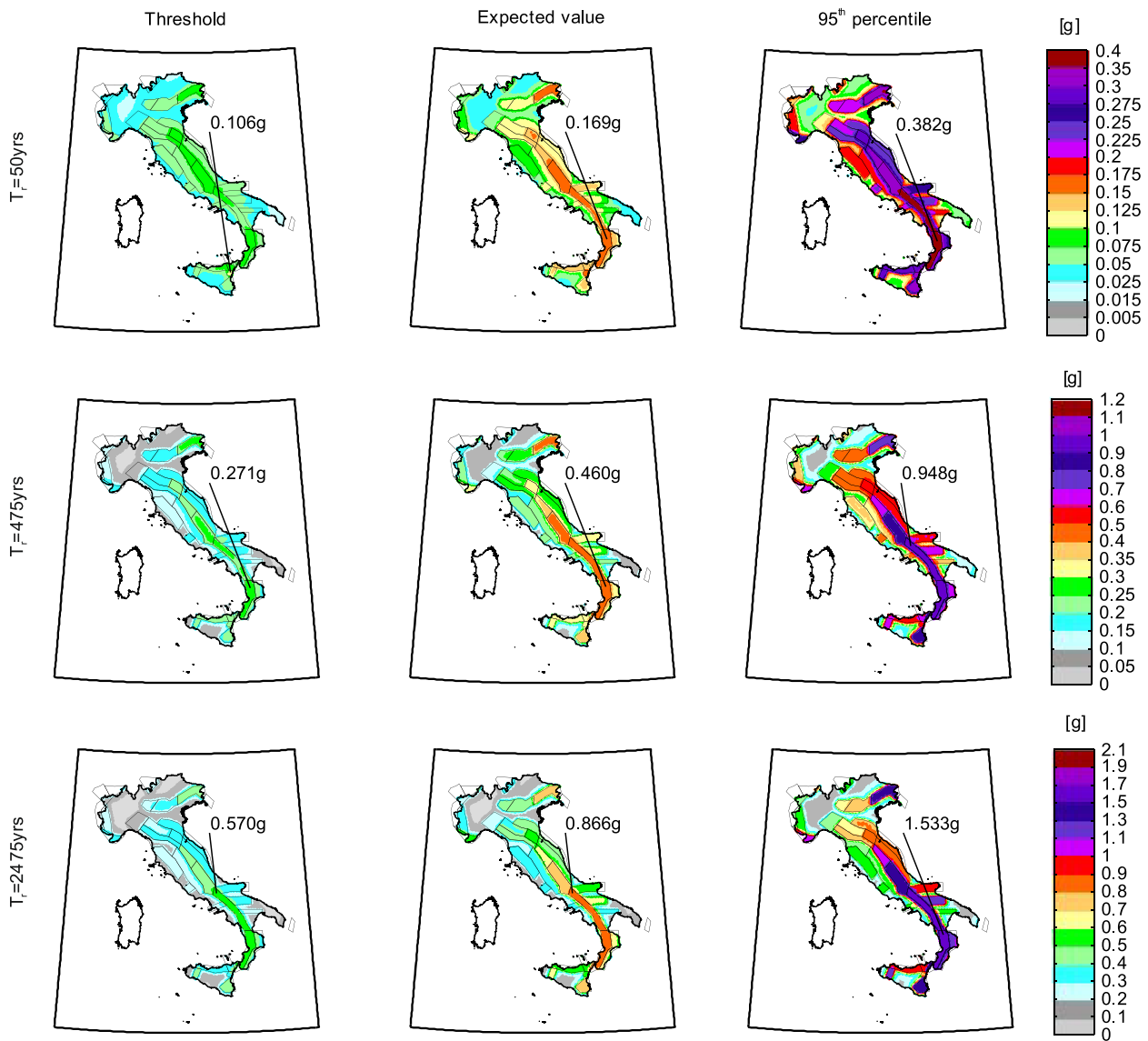
FIGURE 11 Top: Maps of the PGA design threshold, expected value, and 95th percentile of the spectral acceleration given the exceedance of the threshold with 50-year return period at each site; middle is for 475-year return period; bottom is for 2475-year return period

increase in GM due to a 10-fold decrease of the exceedance rate, assuming a linear approximation of the hazard curve. However, the slope does not provide any direct information to quantify the GM beyond design, such as its expected value given exceedance, beyond a linear approximation that may be crude. **As shown, the POT distribution can be computed with the same input information required to compute the slope, that is, the hazard curve alone. Therefore, the POT distribution must be considered preferable in quantifying the GM beyond design at a specific site, being more informative yet computable with the same ease. Nevertheless, because of its widespread use to approximate hazard curves, it may be worthwhile to compare it with the POT. To this aim, using the same national hazard model recalled above, the slope of the hazard curves at the thresholds was computed and mapped for the same return and spectral periods of the POT maps given in the previous section. The maps, given in Figure 13, also provide the absolute value of the mean and the median of the slope across the country.

**As also note that, according to Vamvatsikos[32]: *The most heavily criticized approximation of the SAC/FEMA[33] [reliability] formats is the first-order power-law fit of the hazard curve. It results to unacceptable errors whenever the curvature of the hazard function becomes significant.*
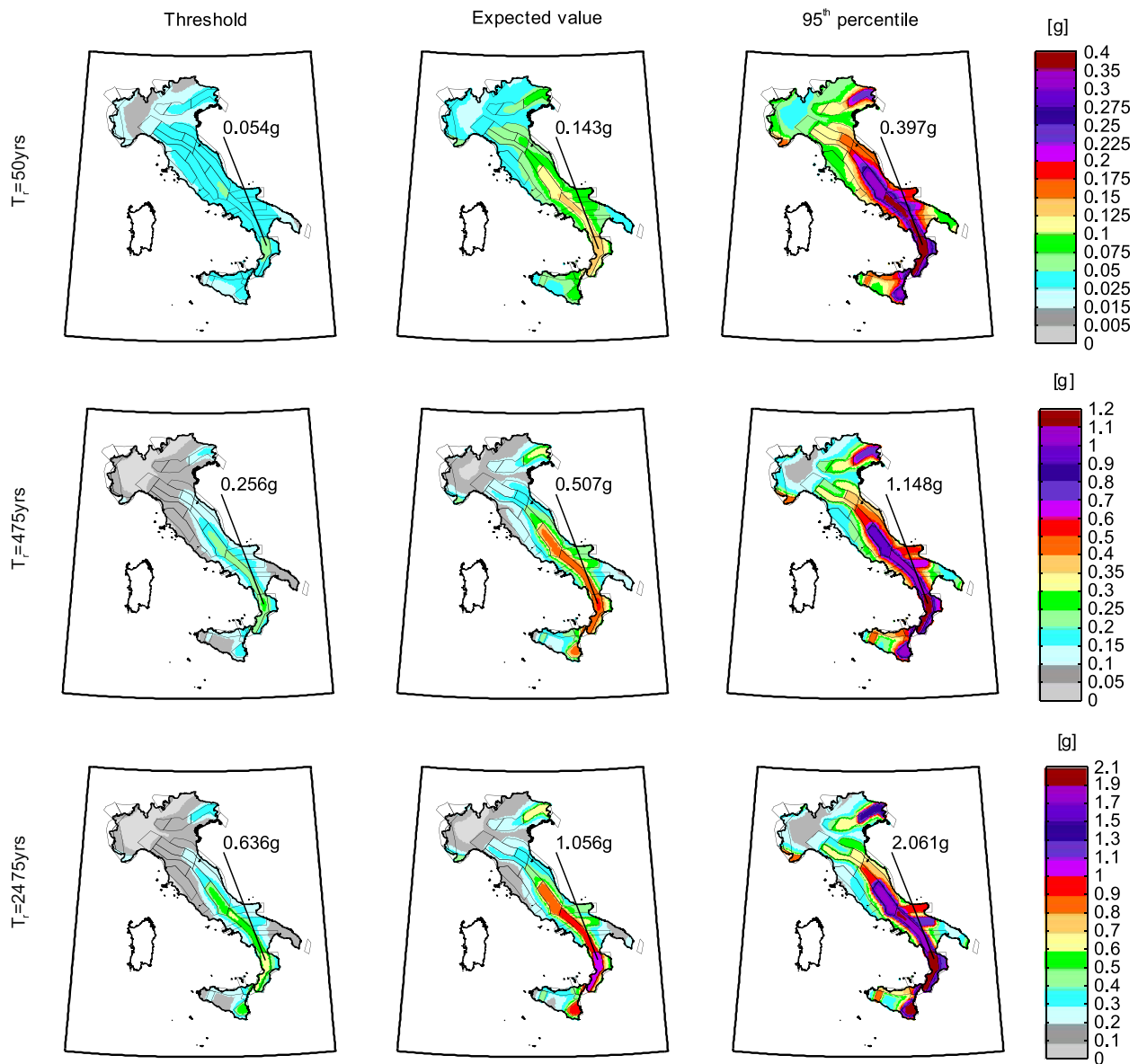
FIGURE 12 Top: Maps of the $Sa(T = 1s)$ design threshold, expected value, and 95th percentile of the spectral acceleration given the exceedance of the threshold with 50-year return period at each site; middle is for 475-year return period; bottom is for 2475-year return period

As expected, the shallower slopes generally correspond to the areas where the POT is larger. However, there are cases in which similar slopes correspond to very different POT. As an example, Figure 14 provides the PGA hazard curves (on rock) for three sites exposed to comparatively low-hazard, mid-hazard, and high-hazard, as it can be seen by the different values of the intensity corresponding to 475-year return period (also given in the figure). While the expected POT increases by a factor of almost four increasing the sites' hazard, the slope is the same. Nevertheless, it should be mentioned that, at least in this example, the slope of the hazard curve is well related to the percentage increase of the POT with respect to the threshold. In fact, for the three sites in the figure, which all have slope equal to 2.3, the ratio of the threshold divided by the expected POT varies between 0.62 and 0.64.

Note that the POT and slope data, the maps given in this paper are based on, are made available at http://wpage. unina.it/iuniervo/papers/POT_maps_Italy.xlsx. In the archive, results are also given for site conditions other than rock; in particular, the POT for other soil classes are computed from those for rock following Equation (6), while the slope of the hazard curve is insensitive to the soil site class.[34]

FIGURE 13 Maps of the hazard curve slope (when plotted in log-log scale) for the three return periods and two spectral ordinates considered
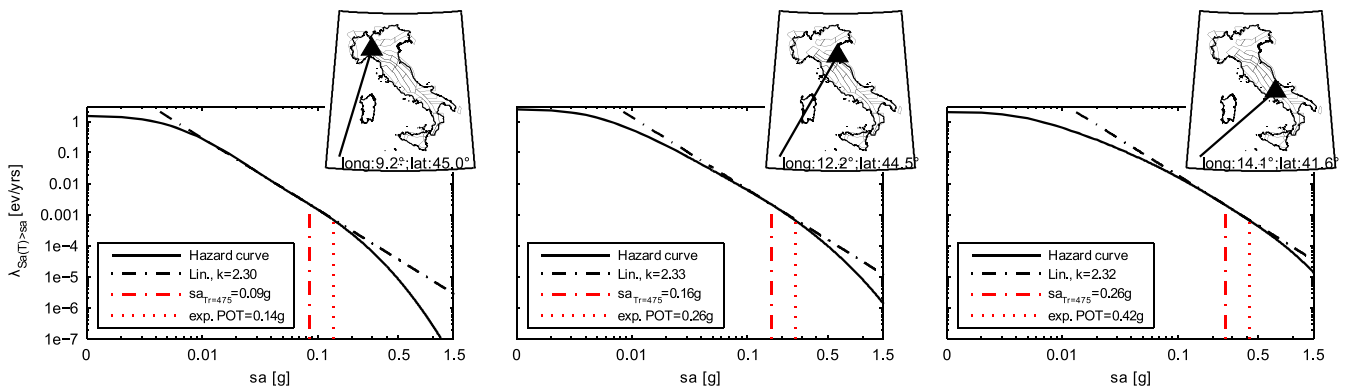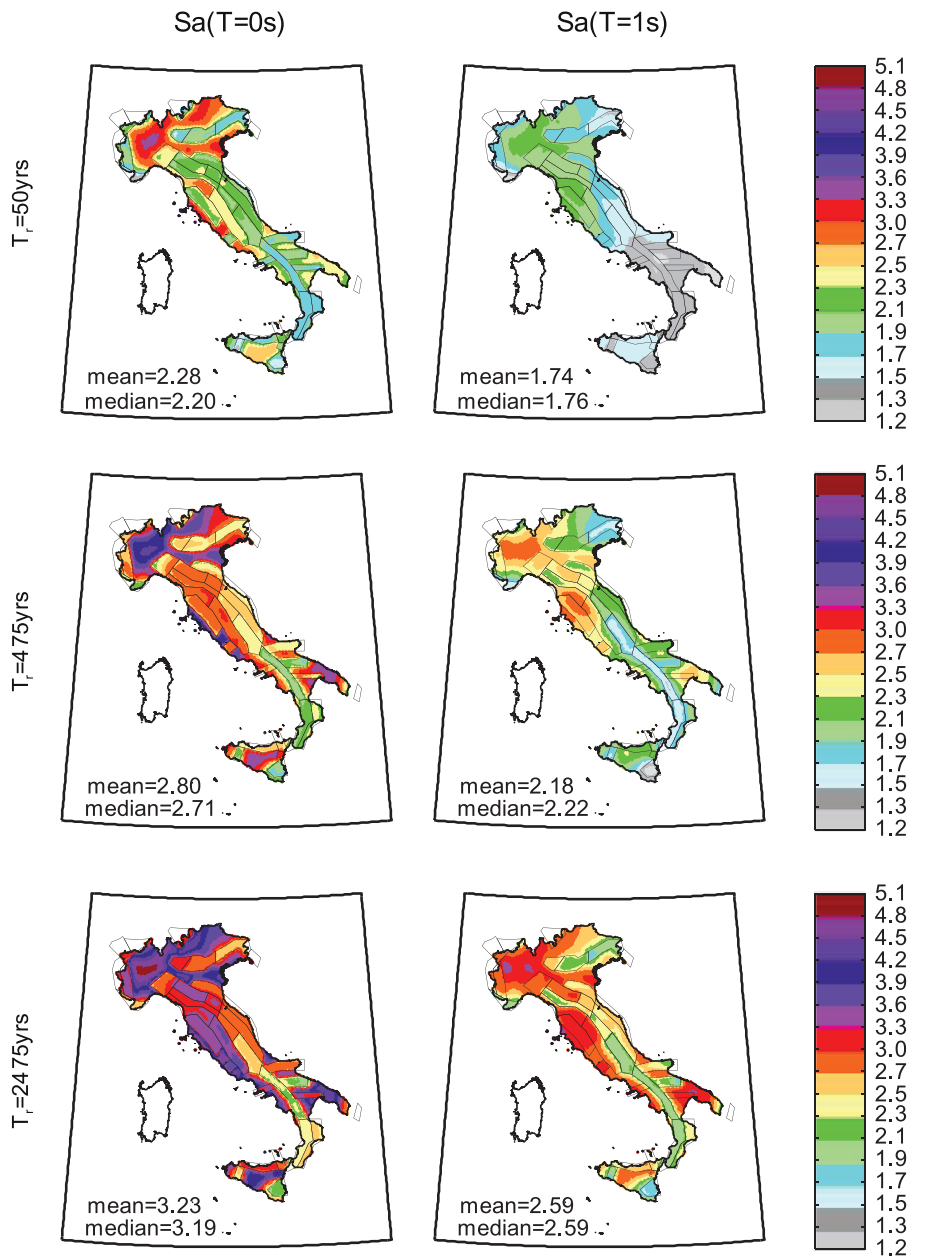

FIGURE 14 Three sites, with significantly different hazard, and then POT, but with similar slope at the threshold

8 | CONCLUSIONS

In performance-based seismic design, actions typically derive from a UHS, the return period of which is based on the limit state of interest. It has been discussed in literature that in the case an earthquake occurs close to the construction site, the design thresholds are likely to be exceeded even for event's magnitude relatively far from the maximum of the sources determining the seismic hazard for the site. From the structural engineering perspective, this means that the design spectrum is not expected to protect in the epicentral areas of these earthquakes, even of relatively moderate magnitude; ie, a code-conforming structure is expected to experience seismic actions beyond those accounted for in design. In this context, the peak-over-the-threshold helps to quantify the (pseudo) accelerations a structure should withstand in the case of strong earthquakes (ie, those able to cause exceedance of the design spectrum).

Extending from previous work, herein, how to compute the full distribution of the POT is discussed. It was shown that such distribution is obtained by truncating the PDF of the spectral acceleration of interest, given the occurrence of one earthquake of unknown characteristics, at the value corresponding to the design threshold. This only requires the derivative of the hazard curve at the site of interest to be computed. Once the distribution of the spectral acceleration over the threshold is available, it allows computing whatever probabilistic measure of the acceleration given exceedance. Moreover, the POT distributions were computed for two spectral ordinates, PGA and $Sa(T = 1s)$, at three (L'Aquila, Milan, and Naples) sites in Italy, referring to three return periods of exceedance of the threshold. This allowed the discussion of the moments and the percentiles as function of site's hazard. The uniform-POT spectra, obtained collecting the expected values and the 95th percentiles of the POT, were also introduced for the sites, as well as POT-conditional-spectra. The POT effect on seismic structural safety was discussed based on some conforming reinforced-concrete moment-resisting frames. Finally, maps of POT percentiles for Italy were given and compared with the corresponding maps of the slope of the hazard curve at the threshold.

The study concluded that the range of actions structures must withstand in earthquakes able to exceed the GM used for design substantially varies with sites' hazard; ie, the percentage difference increases for the most hazardous sites. Moreover, the uncertainty about the actions to be observed in case of exceedance increases as the return period of the exceeded threshold increases (although it decreases relatively to the mean). For example, in the case of the 1-second spectral acceleration at L'Aquila, which is representative of the most hazardous sites in Italy, considering the largest return period the code allows for design (ie, 2475 years), the 95th POT percentile is equal to 172% with respect to the threshold, while the expected POT is 52%. For the same return period, in the case of Milan, which is exposed to relatively lower hazard, percentage differences equal to 38% and 125% were found for the expected value of the peak-over-threshold and the 95th percentile. Naples is in an intermediate situation between the two other sites. The comparison of the spectra-over-the-threshold with the UHS counterparts revealed that the largest absolute differences occur at low-to-mid periods, while maximum percentage increments tend to occur at lower periods.

The Italian POT maps for PGA and $Sa(T = 1s)$ revealed that the average, over the country, of the percentage difference of the expected POT and the threshold are about 70% and 100%, respectively, when the 50-year return period of exceedance is of concern. The average percentage difference considering the 95th POT percentile, for the same return period, are equal to about 230% and 400%, respectively. In the case of the expected POT, these percentage differences reduce to 40% and 50% for PGA and $Sa(T = 1s)$, respectively, when considering the threshold with 2475-year return period. In the case of the 95th percentile, for the same return period, the average percentage differences are equal to about 130% and 200%, for PGA and $Sa(T = 1s)$, respectively.

The comparison of the POT maps with the corresponding map of the slope of the hazard curve, a known proxy for the shape of the hazard curve, showed that it is, as expected, a proxy for the POT; however, the latter can be computed with the same input information needed for the former, and it is more (fully) informative about GM beyond the design value. (All data of the discussed maps, and others, are made available to the interested reader via a linked archive.)

It was also shown that the difference in GMs among sites exposed to different hazard can have a significant effect on the seismic structural safety and is one of the factors why the code-implied structural reliability can be different for structures of the same configuration and typology and designed for the same limits states, yet at different sites. In fact, it was found that, in the analyzed case, the strength reduction factor corresponding to the expected POT in L'Aquila is more than five times that in Milan, while the same reduction factor computed with respect to the design UHS is slighlty less than three times larger for the former site with respect to the latter. Within the approach where design is based on

behavior factors (eg, in Europe), this may call for hazard-dependent strength-reduction and/or for additional performance objectives for those sites where the POT is expected to be larger.

In conclusion, to quantify the GM in earthquakes exceeding the design values can be useful to understand the implications of state-of-the-art seismic design and to interpret the behavior of structures in the epicentral areas of strong earthquakes, where it is likely, by the nature of the design spectra, that actions are larger (several times larger, in the most seismically hazardous sites) than those accounted for in the design process.

ACKNOWLEDGEMENTS

ORCID

Iunio Iervolino https://orcid.org/0000-0002-4076-2718

REFERENCES

1. Cornell CA, Krawinkler H. Progress and challenges in seismic performance assessment. *PEER Cent News*. 2000;3. https://apps.peer.berkeley.edu/news/2000spring/performance.html
2. EN 1998-1. *EN 1998-1—Eurocode 8: Design of Structures for Earthquake Resistance—Part 1: General Rules, Seismic Actions and Rules for Buildings*. Brussels, Belgium: European Committee for Standardization (CEN) 2004.
3. Cornell CA. Engineering seismic risk analysis. *Bull Seismol Soc Am*. 1968;58(5):1583-1606. https://doi.org/10.1016/0167-6105(83)90143-5
4. Reiter L. Earthquake Hazard Analysis: Issues and Insights. *Columbia Univ Press New York*. 1990;254.
5. Luzi L, Pacor F, Puglia R, et al. The Central Italy seismic sequence between August and December 2016: analysis of strong-motion observations. *Seismol Res Lett*. 2017;88(5):1219-1231. https://doi.org/10.1785/0220170037
6. Iervolino I, Giorgio M, Cito P. Which earthquakes are expected to exceed the design spectra? *Earthq Spectra*. 2019;35(3):1465–1483. https://doi.org/10.1193/032318EQS066O
7. Luco N, Hamburger RO, Klemencic M, Seattle A, Jeffrey W, Kimball K. Risk-targeted versus current seismic design maps for the conterminous United States. In: Proceedings of Structural Engineers Association of California (SEAOC) Convetion. Sacramento, CA; 2007.
8. Iervolino I, Spillatura A, Bazzurro P. RINTC project—assessing the (implicit) seimsic risk of code-conforming strutcures in Italy. In: Papadrakakis M, Fragiadakis M, eds. *Proceedings of the 6th International Conference on Computational Methods in Structural Dynamics and Earthquake Engineering (COMPDYN 2017)*. Rodhesisland of Rhodes, Greece; 2017. https://doi.org/10.7712/120117.5512.17282
9. Iervolino I, Spillatura A, Bazzurro P. Seismic reliability of code-conforming Italian buildings. *J Earthq Eng*. 2018;22(suppl 2):5-27. https://doi.org/10.1080/13632469.2018.1540372
10. Iervolino I, Giorgio M, Cito P. The peak over the design threshold in strong earthquakes. *Bull Earthq Eng*. 2019;17(3):1145-1161. https://doi.org/10.1007/s10518-018-0503-9
11. Iervolino I, Chioccarelli E, Convertito V. Engineering design earthquakes from multimodal hazard disaggregation. *Soil Dyn Earthq Eng*. 2011;31(9):1212-1231. https://doi.org/10.1016/j.soildyn.2011.05.001
12. Mc Guire RK. *Seismic hazard and risk analysis*. Oakland, CA: Earthq Eng Res Institute; 2004.
13. Stucchi M, Meletti C, Montaldo V, Crowley H, Calvi GM, Boschi E. Seismic hazard assessment (2003-2009) for the Italian building code. *Bull Seismol Soc Am*. 2011;101(4):1885-1911. https://doi.org/10.1785/0120100130
14. Meletti C, Galadini F, Valensise G, et al. A seismic source zone model for the seismic hazard assessment of the Italian territory. *Tectonophysics*. 2008;450(1-4):85-108. https://doi.org/10.1016/j.tecto.2008.01.003
15. Iervolino I, Chioccarelli E, Giorgio M. Aftershocks' effect on structural design actions in Italy. *Bull Seismol Soc Am*. 2018;108(4):2209-2220. https://doi.org/10.1785/0120170339
16. Ambraseys NN, Simpson KA, Bommer JJ. Prediction of horizontal response spectra in Europe. *Earthq Eng Struct Dyn*. 1996;25(4):371-400. https://doi.org/10.1002/(SICI)1096-9845(199604)25:4<371::AID-EQE550>3.0.CO;2-A
17. Joyner WB, Boore DM. Peak horizontal acceleration and velocity from strong-motion records including records from the 1979 Imperial Valley, California, earthquake. *Bull Seismol Soc Am*. 1981;71(6):2011-2038.
18. Montaldo V, Faccioli E, Zonno G, Akinci A, Malagnini L. Treatment of ground-motion predictive relationships for the reference seismic hazard map of Italy. *J Seismol*. 2005;9:295-316.
19. Bommer JJ, Douglas J, Strasser FO. Style-of-faulting in ground-motion prediction equations. *Bull Earthq Eng*. 2003;1:171-203.
20. Chioccarelli E, Cito P, Iervolino I, Giorgio M. REASSESS V2.0: software for single- and multi-site probabilistic seismic hazard analysis. *Bull Earthq Eng*. 2019;17(4):1769-1793. https://doi.org/10.1007/s10518-018-00531-x

21. Iervolino I, Baltzopoulos G, Chioccarelli E, Suzuki A. Seismic actions on structures in the near-source region of the 2016 central Italy sequence. *Bull Earthq Eng*. 2017;17(10):5429–5447. https://doi.org/10.1007/s10518-017-0295-3

22. van Noortwijk JM, van der Weide JAM, Kallen MJ, Pandey MD. Gamma processes and peaks-over-threshold distributions for time-dependent reliability. *Reliab Eng Syst Saf*. 2007;92(12):1651-1658. https://doi.org/10.1016/j.ress.2006.11.003

23. Artzner P, Delbaen F, Eber J-M, Heath D. Coherent measures of risk. *Math Financ*. 1999;9(3):203-228. https://doi.org/10.1111/1467-9965.00068

24. Iervolino I, Giorgio M, Galasso C, Manfredi G. Conditional hazard maps for secondary intensity measures. *Bull Seismol Soc Am*. 2010;100(6):3312-3319. https://doi.org/10.1785/0120090383

25. Baker JW, Allin CC. Spectral shape, epsilon and record selection. *Earthq Eng Struct Dyn*. 2006;35(9):1077-1095. https://doi.org/10.1002/eqe.571

26. Baker JW, Jayaram N. Correlation of spectral acceleration values from NGA ground motion models. *Earthq Spectra*. 2008;24(1):299-317. https://doi.org/10.1193/1.2857544

27. RINTC-Workgroup. *Results of the 2015-2017 Implicit Seismic Risk of Code-Conforming Structures in Italy (RINTC) Project. ReLUIS Report, Rete dei Laboratori Universitari di Ingegneria Sismica (ReLUIS)*. Naples, Italy; 2018.

28. Ricci P, Manfredi V, Noto F, et al. Modeling and seismic response analysis of italian code-conforming reinforced concrete buildings. *J Earthq Eng*. 2018;22(suppl 2):105-139. https://doi.org/10.1080/13632469.2018.1527733

29. Suzuki A, Baltzopoulos G, Iervolino I, RINTC-Workgroup. A look at the seismic risk of Italian code-conforming RC buildings. In: *Proceedings of 16th European Conference on Earthquake Engineering*. Thessaloniki, Greece; 2018.

30. Fajfar P. Capacity spectrum method based on inelastic demand spectra. *Earthq Eng Struct Dyn*. 1999;28(9):979-993. https://doi.org/10.1002/(SICI)1096-9845(199909)28:9<979::AID-EQE850>3.0.CO;2-1

31. Suzuki A. Seismic fragility assessment of code-conforming buildings in Italy. Ph.D. thesis, Dipartimento di Strutture per l'Ingegneria e l'Architettura, Università degli Studi di Napoli Federico II, Naples, Italy. [Advisor: I. Iervolino] 2019. http://wpage.unina.it/iuniervo/papers/Tesi_Suzuki.pdf.

32. Vamvatsikos D. Derivation of new SAC/FEMA performance evaluation solutions with second-order hazard approximation. *Earthq Eng Struct Dyn*. 2013;42(8):1171-1188. https://doi.org/10.1002/eqe.2265

33. Cornell CA, Jalayer F, Hamburger RO, Foutch DA. Probabilistic basis for 2000 SAC federal emergency management agency steel moment frame guidelines. *J Struct Eng*. 2002;128(4):526-533. https://doi.org/10.1061/ASCE0733-94452002128:4526

34. Iervolino I. Soil-invariant seismic hazard and disaggregation. *Bull Seismol Soc Am*. 2016;106(4):1900-1907. https://doi.org/10.1785/0120160072

CORRIGENDUM

WILEY

Erratum: Peak-over-threshold: Quantifying ground motion beyond design

Pasquale Cito | Iunio Iervolino

There is an error in Equation (12) and in the subsequent description. In fact, Equation (12) should read as:[1]

$$
E\{\log[Sa(T)]\} =
$$
$$
\iint_{M,R} \left\{ \mu_{Sa(T),m,r} + \rho_{T,T^*} \cdot \sigma_{Sa(T)} \cdot \frac{\log\{E[Sa(T^*)|Sa(T^*) > sa_{T_r}]\} - \mu_{Sa(T^*),m,r}}{\sigma_{Sa(T^*)}} \right\} \cdot f_{M,R|Sa(T^*) = E[Sa(T^*)|Sa(T^*) > sa_{T_r}]}(m,r) \cdot dr \cdot dm.
$$

The description of the equation terms should read as follows: ρ_{T,T^*} is the correlation coefficient of the residuals of the GMPEs for the spectral acceleration at the two periods $\{T, T^*\}$.

REFERENCE

1. Cito P, Iervolino I. Peak-over-threshold: quantifying ground motion beyond design. *Earthq Eng Struct Dyn.* 2020;49(5):458-478. https://doi.org/10.1002/eqe.3248

 1